Reduced-scale study of transient flows inside mechanically ventilated buildings subjected to wind and internal overpressure effects

N. Le Roux, X. Faure, C. Inard, S. Soares, L. Ricciardi

Author's manuscript published in Building and Environment, 62, April 2012, pp. 18-32, http://dx.doi.org/10.1016/j.buildenv.2013.01.011

Reduced-scale study of transient flows inside mechanically ventilated buildings subjected to wind and internal overpressure effects

Nicolas Le Roux [a,b,c,*], Xavier Faure [a], Christian Inard [b], Sandrine Soares [c], Laurent Ricciardi [c]

[a] Centre Scientifique et Technique du Bâtiment (CSTB), Nantes, France.
[b] Laboratoire des Sciences de l'Ingénieur pour l'Environnement (LaSIE), La Rochelle, France.
[c] Institut de Radioprotection et de Sûreté Nucléaire (IRSN), PSN-RES, SCA, LEMAC, Saclay, Gif-sur-Yvette, 91192, France.

[*]Corresponding author. Tel.: +33 (0)1 69 08 50 82; Fax: +33 (0)1 69 08 36 80.
E-mail address: nicolas.le-roux@irsn.fr (N. Le Roux).

Abstract

To study transient mass transfers inside buildings equipped with ventilation systems, reduced-scale experiments have been performed by applying the scaling down methodology developed for studying isothermal airflows in a steady or a transient state [1]. Transient tests have been carried out both on simplified cases considered for the validation of the methodology and on two reference industrial configurations representative of real industrial facilities. In this article, focus is made on transient results obtained on simplified and reference industrial cases subjected to wind and internal overpressure effects. The main objectives are firstly to identify the internal transient airflow behaviour, compared with Helmholtz oscillated phenomena underlined from natural ventilation studies, secondly to analyse the pollutant containment of reference industrial configurations subjected to wind and/or internal overpressure effects due to an accident, and finally to check the ability of the SYLVIA code to model these transient phenomena.

Keywords: ventilation systems, dynamic similarity, transient state, Helmholtz resonance, reduced-scale experiments, zonal code SYLVIA

1. Introduction

Buildings equipped with ventilation systems are complex facilities in which steady and transient mass transfers can occur, resulting notably from wind effects or internal overpressures in accidental situations. Predicting these transfers is fundamental to supporting the safety analysis of industrial buildings, and more particularly for facilities containing radioactive materials, such as in the nuclear industry (e.g., power plants, laboratories or nuclear fuel treatment facilities). For these industrial facilities, the main function of the ventilation system is to ensure pollutant containment inside the facility in normal, damaged (ventilation stopped) or accidental situations (e.g., pressure tank fracture, fire or overpressure scenarios), both in steady and transient regimes. To achieve this function, the ventilation system is designed to maintain rooms in depression according to a specific hierarchy from the most to the least hazardous room in terms of contamination. Then, the air, taken from the

outside, flows from the rooms with the lowest contamination risk to the rooms with the highest contamination risk, before being filtered and released into the atmosphere.

For supporting nuclear safety assessments, the zonal code SYLVIA [2] has been developed by the Institut de Radioprotection et de Sûreté Nucléaire to predict steady and transient airflows inside industrial ventilation systems in nominal, damaged or accidental situations. Modelling of airflows due to mechanical ventilation in SYLVIA has already been validated from experiments conducted on real facilities. In addition, the ability of the SYLVIA code to take into account wind effects in steady state has been checked from wind tunnel reduced-scale experiments performed on two reference configurations equipped with ventilation systems and representative of industrial facilities [1]. To do this, a scaling down methodology has been developed for studying both steady and transient airflows inside mechanically ventilated buildings subjected to wind and internal overpressure effects. The theoretical development of the methodology along with the steady-state validation and the steady-state results obtained on both reference configurations are detailed in [1].

No consideration of transient aspects has previously been done and therefore this article focuses on transient results obtained both for the simplified cases considered to validate the scaling down methodology and for the two reference configurations representative of industrial facilities. Section 2 firstly reviews previous reduced-scale approaches developed for studying transient flows, which have been found in the literature only for naturally ventilated buildings [3-6] or train ventilation systems [7]. This underlines the requirement of the specific methodology for industrial ventilation systems developed and summarised in section 2. The presentation of transient results is then divided into two sections: the first one dedicated to results from theoretical and academic cases (section 3) and the second one to results obtained from representative real cases (section 4). Thus, section 3 focuses on transient results obtained for the simplified cases considered to validate the methodology and highlights the influencing parameters, such as inertia and airflow resistances, on the transient airflow behaviour, notably on the emergence of oscillated phenomena. Finally, section 4 presents transient results obtained for the two reference configurations subjected to unsteady wind effects or internal overpressure effects.

2. Previous work

Although the governing equations used to simulate isothermal airflows are quite similar for a single naturally ventilated building and a complex facility equipped with a ventilation system, various reduced-scale approaches were found in the literature depending on the cases studied, the physical phenomena involved and the assumptions considered for ensuring dynamic airflow similarity.

2.1. Dynamic airflow similarity for naturally ventilated buildings

The most theoretical and simplified case consists of a single room with a large opening as illustrated in Figure 1. Holmes [3-4] firstly studied this case because internal pressure fluctuations due to resonance effects may arise in the event of a sudden change of external

pressure generated by strong unsteady wind effects such as in a severe windstorm for example.

Holmes [3] assumed the case studied as a Helmholtz resonator and developed the first reliable model taking into account internal pressure fluctuations, by integrating inertial effects through the opening and air compressibility effects inside the room, expressed as the following non-linear second-order equation

$$\frac{\rho L_e V}{\gamma P_0 S}\frac{d^2 C_{P\text{int}}}{dt^2}+\left(\frac{\rho V U}{2C_D \gamma P_0 S}\right)^2 \frac{dC_{P\text{int}}}{dt}\left|\frac{dC_{P\text{int}}}{dt}\right|+C_{P\text{int}}=C_{Pext} \qquad \textbf{Eq. 1}$$

where C_{Pint} and C_{Pext} are the internal and external pressure coefficients (-) defined as the ratio between relative and upstream dynamic pressures, ρ is the reference density of air (kg.m^{-3}), γ is the polytropic exponent (-), C_D is the discharge coefficient (-), U is the mean upstream wind velocity (m.s^{-1}), P_0 is a reference static pressure (Pa) usually defined as the atmospheric pressure, V is the room volume (m^3), S is the opening section area (m²) and L_e is the effective length of the air moving through the opening (m) given by [8]

$$L_e = L + 0.89\sqrt{S} \qquad \textbf{Eq. 2}$$

where L is the opening length (m). Thus, Holmes [3] showed that the internal pressure oscillations correspond to Helmholtz oscillations, the undamped resonant frequency f_H (Hz) of which, given by Eq. 3, increases as the room volume decreases and the opening section area increases.

$$f_H = \frac{1}{2\pi}\sqrt{\frac{\gamma P_0 S}{\rho L_e V}} \qquad \textbf{Eq. 3}$$

A similar model has been developed by Liu et al. [9] from the unsteady fluid mechanics equations and much research was then carried out to numerically and experimentally study Helmholtz oscillations inside a dominant windward opening building (e.g., Refs. [10-13]). To experimentally reproduce internal pressure oscillations at a reduced scale, Holmes [3] defined a dynamic similarity criterion, from a dimensionless form of Eq. 1, which should be ensured between the full scale and the reduced scale. In terms of scale parameters between both scales, the conservation of this dynamic similarity criterion is written as

$$\overline{V} = \frac{\overline{L}^3}{\overline{U}^2} \qquad \textbf{Eq. 4}$$

where $\overline{V}$, $\overline{L}$ and $\overline{U}$ are respectively the room volume scale, the opening length scale and the velocity scale, defined as the ratio between the reduced-scale and the full-scale variables. Eq. 4 shows that if a velocity reduction is considered for reduced-scale experiments ($\overline{U} \neq 1$), the room volume scale is not equal to the opening volume scale and thus a volume distortion between the room and the opening is introduced. Oh et al. [13] reviewed reduced-scale

experiments sized up by considering this volume distortion (e.g., Refs. [14-17]) or not (e.g., Refs. [10, 12, 18]). Introducing this volume distortion is only necessary to correctly reproduce the frequencies of internal pressure fluctuations in the case of Helmholtz oscillations [3-4]. Knowing that ensuring the volume distortion might be challenging, identifying which parameters have an influence on these oscillations is fundamental and needs more detailed research work. For example, experiments were carried out to study the influence of building leakage and envelope flexibility and have shown that both parameters decrease the resonance effects [19-20].

In addition, to study naturally ventilated buildings composed of several openings subjected to steady and unsteady wind effects, and more precisely to wind turbulence effects, Etheridge [5-6] developed a similar dimensionless model, which leads to an analogous dynamic similarity criterion. For such a case, Chiu [21] showed that internal fluctuations, generated by wind turbulence, obtained with models designed with and without considering the volume distortion were quite similar and thus the dynamic similarity criterion should not necessarily be ensured. Consequently, wind tunnel tests for studying the wind turbulence influence were performed without considering the volume distortion theoretically needed from the similarity study [22].

Hence, considering the volume distortion for designing reduced-scale models clearly depends on the internal phenomena identified, which depend on the characteristics of the cases studied and on the phenomena studied (e.g., wind turbulence effects, severe transient disturbance due to an accident). Thus, knowing that the volume distortion is also imposed by the methodology developed for mechanically ventilated buildings [1], investigation is needed to identify for which cases the Helmholtz resonant effects may arise for complex buildings composed of several rooms, ventilation systems and leaks.

2.2. Dynamic similarity for ventilation systems

A reduced-scale approach for studying transient flows inside installations equipped with ventilation systems was only found for train ventilation systems [7] and cannot be extended to carrying out wind tunnel reduced-scale experiments for industrial buildings (section 2.2.1). For this reason, a specific methodology for mechanically ventilated buildings has been developed by Le Roux et al. [1], the development of which is summed up in section 2.2.2.

2.2.1. Train ventilation systems

When a train goes through a tunnel, high overpressures and depressions, characterized by approximately 2000 Pa in 1 second, are generated on the external walls of the train. These transient variations lead to a sudden change of the train internal pressure, due to the propagation of the pressure fluctuations inside the ventilation system. To study the feasibility of a device monitoring the instantaneous flow rates inside the ventilation system and thus decrease the harmful effects inside the train, Mariaux [7] developed a scaling down approach for experimentally reproducing this transient phenomenon inside a simplified train ventilation system, as illustrated in Figure 2.

As for natural ventilation approaches, the methodology is based on fluid mechanics equations expressed in a dimensionless form, namely the mass conservation equation applied in nodes (i.e. the train volume and the junction P_A) and the integral kinetic energy theorem applied in the four ventilated branches. However, the main assumption used to define the dimensionless model is that the sound velocity is considered as the reference velocity and then all reference variables are written depending on the sound velocity. In addition, Mariaux [7] imposes similar reduced-scale and full-scale times, i.e. the time scale is set at one. Thus, the similarity study leads to the following two expressions between scale parameters

$$\overline{U} = \overline{P} = \overline{L} = \overline{t} = 1 \qquad \textbf{Eq. 5}$$

$$\overline{Q} = \overline{S} = \overline{V} \qquad \textbf{Eq. 6}$$

where $\overline{V}$ is the train volume scale, $\overline{L}$ is the branch length scale, $\overline{S}$ is the branch section area scale, $\overline{U}$ is the velocity scale, $\overline{P}$ is the pressure scale, $\overline{Q}$ is the volumetric flow rate scale and $\overline{t}$ is the time scale.

Given that the sound velocity is identical whatever the scale, the velocity cannot be modified and consequently no volume distortion is theoretically needed, i.e. the train volume scale ($\overline{V}$) is equal to the branch volume scale ($\overline{S}\overline{L}$). Then, due to the expressions of their reference variables depending only on parameters (sound velocity, reference constant time), the pressure scale, the length scale and the time scale should also be equal to one. Satisfying Eq. 5 is very constraining, notably for designing reduced-scale models inside a laboratory with similar branch lengths between the full-scale and the reduced-scale models. However, Mariaux [7] numerically showed that the branch lengths, and consequently the branch inertia, have no influence on the pressure propagation for the case studied (Figure 2). The reduced-scale train ventilation system was thus designed without ensuring the length scale and arbitrary reduced-scale lengths were considered, meaning that the train ventilation system inertia was neglected.

In addition, satisfying Eq. 6 is also constraining for large industrial buildings because the room volume should be considerably reduced to design models and the reduced-scale flow rates should not be too low, notably due to the measurement uncertainties. Finally, knowing

that the pressure scale is equal to one, the flow-rate reduction should not be too low in order to find appropriate fans and reproduce head losses.

2.2.2. Buildings equipped with ventilation systems

The main principle of the methodology developed by Le Roux et al. [1] for mechanically ventilated buildings, taking into account the whole building characteristics including the ventilation system and its inertia, is summarised below. Details regarding the development of the methodology can be found in Le Roux et al. [1] and Le Roux [27].

First, the dimensionless model, given by the integral kinetic energy theorem for passive branches (Eq. 7) and the mass balance equation for nodes (Eq. 8), has been developed by introducing dimensionless variables for all physical and geometrical variables. For fans, specific models exist in which the fan curve is considered as an input data. Thus, the similarity of fans will be based on the conservation of the fan curves by applying the pressure and the flow rate scales to the real fan curves.

The dimensionless variables X^* are expressed as the ratio between the variable X and its reference value X_{ref} for each variable, namely the node pressure P (Pa), the volumetric flow rate Q (m^3/h), the air density ρ (kg/m^3), the time t (s), the room volume V (m^3), the branch length L (m), the branch section area S (m^2) and the airflow resistance R ($kg^{(2-n)}/m^4/s^{(2-n)}$) representing the head losses of each branch. Note that the reference pressure, the reference flow rate and the reference time are expressed from the other reference variables [1]. In Eq. 8, i and j respectively represent the subscripts for inlet and outlet flows and P_{atm} is the atmospheric pressure (Pa).

$$\frac{\rho^* L^*}{S^*}\frac{dQ^*}{dt^*} = \Delta P^* - \underbrace{\left[\frac{R_{ref} S_{ref}^n}{\left(\rho_{ref} U_{ref}\right)^{2-n}}\right]}_{N_1} \rho^{*n-1} R^* \,\mathrm{sgn}\left(Q^*\right)\left|Q^*\right|^n \qquad \textbf{Eq. 7}$$

$$\frac{dP^*}{dt^*} = \underbrace{\left[\frac{P_{atm}}{\rho_{ref}}\frac{S_{ref} L_{ref}}{V_{ref} U_{ref}^2}\right]}_{N_2} \frac{\sum_i \rho_i^* Q_i^* - \sum_j \rho_j^* Q_j^*}{V^*} \qquad \textbf{Eq. 8}$$

Eq. 7 can be defined in three forms depending on the branch type (duct, filter or leak), for which the exponent n is respectively considered as 1 for a filter, 2 for a duct and between 1 and 2 for a leak. Values between 1.35 and 1.7 are usually found in the literature [13, 23-24]. Thus, the dimensionless model reveals the dimensionless parameter N_1, written under three different forms depending on the type of branch, and the dimensionless parameter N_2. In terms of scale parameters between a full scale and a reduced scale, the conservation of these two dimensionless parameters is written as

$$\overline{R} = \frac{\overline{U}^{2-n}}{\overline{S}^{n}} \qquad \textbf{Eq. 9}$$

$$\frac{\overline{S}\,\overline{L}}{\overline{V}\,\overline{U}^{2}} = 1 \qquad \textbf{Eq. 10}$$

where $\overline{R}$ is the airflow resistance scale, $\overline{U}$ is the velocity scale, $\overline{S}$ is the branch section area scale, $\overline{L}$ is the branch length scale and $\overline{V}$ is the room volume scale. Thus, the airflow resistance scale of the three types of passive branches can be determined from Eq. 9 if the velocity and the section scales are known. Eq. 10 is similar to the dynamic similarity criterion Eq. 4 defined by Holmes [3] if a branch section area scale equal to the square of the branch length scale is considered ($\overline{S} = \overline{L}^{2}$).

Table 1 sums up the relations between the fixed and the calculated scale parameters, showing that several sets of scale parameters can be defined depending on the cases studied and the hypotheses considered. From the conservation of the dimensionless parameters (Eqs. 9 and 10) and the relations between reference variables, seven relations given in Table 1 are used to define the scale parameters. Knowing that ten scale parameters should be determined, the scaling down methodology consists in fixing the three most constrained scale parameters, i.e., the room volume scale, the flow rate scale and the velocity scale. The choice of these parameters is mainly constrained by the real configuration characteristics and the experimental means [1].

The methodology has then been numerically and experimentally validated on simple configurations by comparing results obtained from full-scale models and reduced-scale models, defined from a set of scale parameters according to the theoretical development above. Steady-state validation is given in Le Roux et al. [1] and the main transient results of the validation are explained in section 3.

Thus, in theory, to rigorously ensure transient airflow similarity inside buildings equipped with ventilation systems, reduced-scale models must be designed by introducing a volume distortion between the branches and the rooms, except if the velocity is not reduced between the full scale and the reduced scale. However, it has been shown from natural ventilation studies that the volume distortion is necessary only if internal oscillations, corresponding to Helmholtz resonance, occur (e.g., [21-22]). The necessity of considering this volume distortion for mechanically ventilated buildings depends on the transient airflow behaviour, which will be characterized for the simplified cases in section 3 and for the reference industrial cases in section 4.

3. Analysis of transient flows for simplified cases

In this section, the impact of the volume distortion and the influence of the branch inertia on the transient airflows are firstly highlighted from the simplified cases studied to validate the scaling down methodology. The influence of branch characteristics, namely the inertia and the

airflow resistance, is then rigorously characterized from a parametrical study conducted for a simplified theoretical case.

3.1. Simplified cases studied

The simplified cases studied are composed of one room, one blowing branch and one exhaust branch, as illustrated in Figure 3. Numerical and experimental cases were studied at two scales, by applying scale parameters defined from the methodology developed.

First, for the numerical verification of the methodology (section 3.2.1), models were considered at a full scale and a reduced scale, defined by considering a room volume scale of $1/12^3$, a velocity scale of $1/\sqrt{2}$ and a flow rate scale of 1/80 and by applying the relations given in Table 1. These scale parameters correspond to those defined for designing the two reference industrial cases and were also considered in order to numerically validate the methodology with representative full-scale and reduced-scale characteristics. The choices of these scale parameters depend on the experimental constraints and full-scale characteristics of the reference industrial cases [1]. For the numerical validation, a room volume of 12 x 12 x 12 m^3 and branches of 50 m length and 0.6 m diameter were considered for the full-scale numerical models.

For the experimental validation of the methodology (section 3.2.1), the scale parameters and full-scale characteristics used for the numerical verification and for the industrial cases studied thereafter cannot be used for experimental models. Thus, another set of scale parameters was defined by considering a room volume scale of $1/3^3$, a velocity scale of $1/\sqrt{2}$ and a flow rate scale of 1/27. Considering this set of scale parameters, a reference-scale model and a reduced-scale model have been sized up in the laboratory by ensuring the similarity between both scales. In addition, corresponding numerical models were defined for each experimental model in order to compare experimental and numerical transient results. A room volume of 0.9 x 0.9 x 0.9 m^3 and ducts of 2.24 m length and 192 mm internal diameter were considered for the reference-scale model (Figure 4). Each model was equipped with pressure taps at the inlet of the blowing duct, inside the room, and on each side of orifice plates located inside the exhaust ducts for the volumetric flow rate measurements. Specific orifice plates, for which pressure taps are symmetrically positioned right next to the orifice plate, were designed according to the AFNOR NFX 10-231 standard [25]. In addition, pressures were recorded by PSI sensors at 200 Hz with appropriate tubing systems designed to act as a low-pass filter over the required frequency range [26], for which the uncertainties are approximately equal to ± 2.5 Pa. Note that for pulsating flows, many factors may affect the accuracy of the instantaneous flow rate measurements if they are not taking into account, notably the temporal inertia, the flow direction inside orifices, the nonlinearity of the law and the pressure measurement system [29]. These ones were considered while estimating transient flow rates, except the temporal inertia due to its low influence for the transient cases studied. In addition, note that the main transient results presented in this paper are given in terms of pressures.

In addition, for experimentally studying the influence of inertia on the transient airflow behaviour, “inertial” models were designed by increasing the blowing duct length.

Experimental cases are presented in Figure 4 and the branch properties are given in Table 2. Note that inertia is defined as the ratio $\rho L/S$ from the integral kinetic energy theorem for branches (dimensionless form given by Eq. 7), where L and S are respectively the duct length and the duct section area and ρ is considered as the reference density. These "inertial" models were designed only for studying the inertia influence on each model, but without ensuring the scale parameters between both scales.

3.2. Validation of the methodology for transient flows

Only the main transient results, which characterize the internal airflow behaviour inside simplified cases, are presented herein but further details regarding the validation can be found in Le Roux [27] or Le Roux et al. [28].

3.2.1. Numerical verification of the methodology

Numerical verification was carried out both considering the dimensional model with the SYLVIA code and the dimensionless model by implementing the model developed, given by Eqs. 7 and 8, in the Matlab Software. Transient simulations have been performed by considering a pressure peak at the inlet of the blowing branch as boundary condition. The full-scale pressure amplitude and duration are respectively equal to 1000 Pa and 4 s, and the corresponding reduced-scale pressure peak is obtained by applying the pressure scale ($\overline{P} = 1/2$) and the time scale ($\bar{t} \approx 1/43.2$) defined from Table 1. Thus, the reduced-scale pressure amplitude and duration are respectively equal to 500 Pa and 0.093 s.

Room pressures and flow rates obtained at both scales and with both numerical approaches have been compared at the full scale, after the transposition of the reduced-scale results to the full scale by applying the corresponding scale parameters. An example of full-scale comparisons between full-scale and reduced-scale results is presented in Figure 5. In addition, results obtained on a reduced-scale model defined without introducing the volume distortion imposed by the scaling down methodology are also presented in Figure 5. Instead of considering Eq. 10, geometrical scale parameters were defined by assuming $\overline{V} = \overline{S}\overline{L}$. Thus, the reduced-scale models designed with and without the volume distortion differ only in the room volume respectively equal to 1 m^3 and 0.5 m^3. The ratio between both volumes logically corresponds to the square of the velocity scale (Eq. 10).

Figure 5 shows that full-scale results and reduced-scale results, transposed to the full scale by strictly ensuring the scaling down methodology, are similar. By contrast, reduced-scale results obtained without considering the volume distortion are considerably different during transient variations of pressures and flow rates. Thus, considering the volume distortion, which is required for ensuring transient airflow similarity if the velocity scale is not equal to one, is fundamental for studying reduced-scale transient flows inside this type of simplified configuration. It is also worth noting that overshoot appears before reaching the steady-state blowing flow rate. By analogy with Helmholtz oscillations identified for a room with a single opening [3-4], this overshoot could be considered as oscillations associated with a high damping ratio.

3.2.2. Experimental validation of the methodology

Experimental tests have been carried out by generating overpressures at the inlet of the blowing branch by using an air valve controller connected to the pressure air plant of the laboratory. With this device, it was difficult to rigorously ensure the similarity of these transient inlet pressures. In addition, note that "inertial" models were designed without ensuring the similarity, which implies that experimental results between both scales cannot be compared. For these reasons, experimental results were compared with numerical results for each model studied, knowing that the methodology has already been numerically validated. Note that the aim of these tests was also to experimentally underline the influence of inertia on the internal transient airflow behaviour. Thus, the experimental inlet pressures were used as boundary conditions for numerical simulations. Figure 6 presents the inlet overpressures and compares the corresponding experimental and numerical room pressures obtained for the reference-scale, the reduced-scale and the second "inertial" reduced-scale models (Table 2). Only this last inertial model, corresponding to the most inertial case, is presented.

Figure 6 shows that experimental and numerical results are in good agreement for each model considered, even if the inertia of the blowing duct is considerably increased. It is particularly worth noting that numerical results reproduce the oscillations underlined from experiments. Oscillations are identified at a frequency of approximately 4.7 Hz and 12.5 Hz in the reference-scale and the reduced-scale models, respectively, whereas oscillations are not identified for the most inertial case (e.g., the "inertial" reduced-scale model n°2). As for natural ventilation cases presented in the literature [3], these frequencies correspond to Helmholtz frequencies and depend on the characteristic sizes of each model. From the parametrical simulations presented below, it will be shown that the analytical expression of the undamped Helmholtz frequency (Eq. 3) is valid to calculate the frequency values if the damping ratio is significantly lower than unity.

Note also that the temporal phase differences between the inlet pressures and the room pressures remain very low, even for the most inertial case for which a maximal temporal phase of approximately 0.2 second is identified between the inlet and room pressure peaks. From these experiments, the temporal phases and the damping ratio of oscillations seems to be linked to the inertial properties but also to the branch airflow resistances. Attempting to draw conclusions on the influence of inertia and airflow resistance on such transient phenomena from these tests is difficult because both parameters are related by the friction head losses inside ducts. For this reason, a parametrical analysis is presented in section 3.3, which enables the influence of each parameter to be studied separately.

3.3. Parametrical study of the influence of inertia and airflow resistances

The parametrical study has been done on a full-scale simplified case as illustrated in Figure 3, by considering quadratic branches, i.e. branches associated with a quadratic law (Eq. 7 with an exponent n equal to 2) notably used to model turbulent ventilated ducts, which are the main inertial components of a ventilation system. However, by firstly considering linear blowing and exhaust branches, i.e. branches associated with a linear law (Eq. 7 with an exponent n

equal to 1) usually used to model HEPA filters, with similar properties, an analytical case can be determined and enables the characteristic quantities of the transient internal pressure evolution to be defined theoretically.

3.3.1. Theory for linear branches

The transient evolution of the internal pressure inside a single room with linear blowing and exhaust branches with similar properties (inertia and airflow resistances), is modelled by a second-order linear equation

$$\frac{d^2 P_{room}}{dt^2} + 2\xi\omega_n \frac{dP_{room}}{dt} + \omega_n^2 P_{room} = K\omega_n^2 P_{inlet} \qquad \textbf{Eq. 11}$$

The characteristic parameters, namely the undamped natural frequency ω_n (Hz), the damping ratio ξ and the static gain K are written as

$$\omega_n = \sqrt{\frac{2rT}{M}\frac{S}{LV}} \qquad \xi = \frac{R}{2}\sqrt{\frac{1}{2}\frac{M}{\rho^2 rT}\frac{SV}{L}} \qquad K = \frac{1}{2} \qquad \textbf{Eq. 12}$$

where L, S and R are respectively the length (m), the section (m²), and the linear airflow resistance (kg.m^{-4}.s^{-1}) equal for both branches, V is the room volume (m^3), M is the molecular mass of air (kg/mol), r is the perfect gas constant (8.314 J/mol/K), T is the ambient temperature (293.15 K), ρ is the air density (kg/m^3) assumed as similar inside the room and the branches. For such a model, the pseudo-periodic state, reached when the damping ratio ξ is lower than unity, is characterized by the following quantities: the oscillation frequency f, the first peak overshoot D_1, the response time T_r and the rise time T_m between 10 % and 90 % of the steady-state value. These quantities are illustrated in Figure 7 for a pseudo-periodic evolution of the room pressure as a result of a pressure step at the inlet of the blowing branch.

Analytical solutions of the characteristic quantities can be determined for a linear equation, notably the oscillation frequency f (Hz), which is given by:

$$f = \frac{\omega_n\sqrt{1-\xi^2}}{2\pi} \qquad \textbf{Eq. 13}$$

Thus, if the damping ratio is significantly lower than unity, the oscillation frequency only depends on the undamped natural frequency ω_n. In this case, the frequency is proportional to the inverse of the square root of the inertia and room volume product (Eq. 12). Note that the frequency is independent of the airflow resistance only if the damping ratio is negligible. This damping ratio is both proportional to the airflow resistance and inversely proportional to the square root of the branch inertia (Eq. 12). Thus, for low airflow resistances, the oscillation frequency only depends on the inertia, except if this is also very low. By contrast, the aperiodic state, i.e. the regime without oscillations corresponding to a damping ratio higher than unity, is reached by increasing the airflow resistance or decreasing the inertia.

Due to the non-linearity of the model when quadratic branches are considered, conclusions cannot be drawn from analytical expressions for cases with ventilated ducts and thus parametrical simulations were performed with quadratic branches.

3.3.2. Results of parametrical simulations for quadratic branches

Parametrical simulations have been performed by independently modifying the airflow resistances and the inertia of branches. These parameters can be considered as independent because ventilation systems are composed of several components (e.g., bends, reductions, dampers), which introduce large singularity head losses in addition to friction head losses. The room volume and the branch diameter were set at 5 x 5 x 5 m^3 and 0.2 m, respectively. The properties of both ducts were simultaneously changed: the airflow resistances varied from 10 to 100 000 m^{-4} and the inertia was changed by considering four different lengths (1, 10, 50 and 100 m), corresponding to inertia values from 38 to 3800 $kg.m^{-4}$, approximately. In terms of dimensionless parameters, and for generalising these results to other future studies, these variations lead to variations from 2.5 10^{-4} to 2.5 10^{+2} for the dimensionless number N_2 and from to 0.01 to 100 for the dimensionless number N_1 similar for both ducts due to their similar properties.

Figure 8 presents the characteristic quantities of the time response of the system studied as a function of airflow resistance for the four duct lengths considered. The oscillation frequency graph enables the aperiodic and the pseudo-periodic regimes to be distinguished: for the aperiodic regime, no frequency can be calculated and thus no points are plotted on the curves.

Similar conclusions to those obtained for the linear analytical case are obtained from Figure 8. First, the oscillation frequency graph shows that the threshold between the pseudo-periodic and the aperiodic regimes, analytically characterized by the damping ratio (section 3.3.1), increases as the inertia increases and the airflow resistance decreases. Thus, the probability of reaching the pseudo-periodic regime increases when the airflow resistance decreases and the inertia increases. The oscillation frequency increases when the inertia decreases and depends only on inertia under a threshold value of airflow resistance. However, these threshold values also depend on the inertia and correspond to a damping ratio significantly lower than unity as it has been concluded for the analytical case.

In addition, Figure 8 shows that the response time is logically increased in the case of high oscillations and more particularly when the damping ratio is low, corresponding to low airflow resistances and high inertia. Moreover, the first peak overshoot graph shows that the oscillations amplitude increases when increasing the inertia, which can notably reach a peak of approximately 100 % of the steady-state value when the airflow resistance is low.

Finally, one main conclusion is that for airflow resistances higher than 5000 m^{-4}, the aperiodic regime is reached, because higher the airflow resistance is, higher the damping ratio is. In this regime, the influence of inertia on the response time is very low and thus the branch inertia can be neglected. To conclude, if the aperiodic regime is identified in real configurations, the branch inertia can be neglected and thus the conservation of branch section scale and branch length scale is no longer necessary. Consequently, no volume distortion should be ensured

between rooms and branches because only one geometrical reduction for rooms should be considered. This conclusion is based only on the analysis of simplified configurations and thus needs to be validated on reference industrial configurations before applying this simplification when using the scaling down methodology.

In principle, knowing that the global airflow resistance of real ventilation systems is higher than the resistance of the simplified cases and the naturally ventilated cases of the literature for which oscillations have been identified, oscillated phenomena may not appear inside reference industrial cases. However, this will be studied in the following section and it will be shown that overshoot phenomena corresponding to high damping oscillations could arise in some specific conditions.

4. Analysis of transient flows for reference industrial configurations

Steady and transient flows have been experimentally and numerically studied on two mechanically ventilated facilities subjected to wind and/or accidental overpressure effects. Wind tunnel experiments were carried out in the Jules Verne climatic wind tunnel of the CSTB, on the two reference industrial configurations briefly summarised in section 4.1. Focus is herein made on transient phenomena by firstly analysing the wind turbulence effects on the containment of pollutants inside buildings (section 4.2) and secondly studying internal overpressure effects due to an accident (section 4.3). Note that the results presented in this section are systematically given at the full scale, by applying the corresponding scale parameters to the reduced-scale results.

4.1. Reference industrial cases studied

Figure 9 presents the building architecture of both configurations studied, each one composed of four rooms linked with a ventilation system and leakages between rooms and with the outside, corresponding mainly to the airtightness defects of the building's doors. The first configuration represents a facility in high interaction with the outside, whereas the second one corresponds to a more realistic nuclear facility due to the interlocking of rooms, such that only the least hazardous room, in terms of contamination, is linked to the outside.

The ventilation system of both configurations is composed of three fans, six HEPA filters and about twenty ventilated ducts with singularities, such as bends, reductions and control dampers. The standard real size of ducts in ventilation systems typically ranges from 10 to 100 m in length and from 0.2 to 1.0 m in diameter. Thus, by considering these standard values for the design of both configurations, the inertia of each duct varies from 8 to 1280 $kg.m^{-4}$. For the airflow resistances of branches, full-scale numerical values calculated from the nominal pressures and flow rates reach a maximum of about 12 000 m^{-4} for quadratic branches, 11 600 $kg.m^{-4}.s^{-1}$ for linear branches and 121 450 $kg^{(2-n)}.m^{-4}.s^{(n-2)}$ for leaks.

For each configuration, a reduced-scale model has been sized up by applying relations given in Table 1 considering a room volume scale of $1/12^3$, a velocity scale of $1/\sqrt{2}$ and a flow rate scale of 1/80. Details regarding the full-scale configurations and the reduced-scale models are

given in Le Roux et al. [1]. Both configurations were equipped with more than 130 pressure taps where the pressure is recorded by PSI sensors at 200 Hz. The pressure was measured at each internal node (rooms and junctions between the ducts) and each boundary condition node (external pressure measured at the ventilation system inlet, the exhaust chimney outlet and the outside of each external leak). Pressure taps were also located right next to the orifice plates upstream and downstream to determine the volumetric flow rates inside the ducts according to the AFNOR NFX 10-231 standard [25]. The volumetric leakage flow rates were measured using the calibrated laws of each perforated plate. As mentioned in section 3.1, factors affecting the measurement of transient flow rates were taken into account [29], except the temporal inertia due to its low influence identified across the orifice plates. Before studying wind and internal overpressure effects, models have been characterized by studying the airflow behaviour of each component (fans, ventilated ducts, leaks, filters) and the hierarchy of depressions between rooms, given in Figure 9, has been checked in nominal situations [27].

4.2. Wind turbulence effects

4.2.1. Experimental characterization of instantaneous leakage flow rate inversions

Wind generates overpressures and depressions on the external communications of the facility, namely the ventilation system inlet, the exhaust chimney and the external leaks, and consequently modifies internal airflows. From the steady-state analysis [1], it has been shown that the wind influence is the most significant on the leakages of rooms, for which flow inversions could occur depending on the operation of the mechanical ventilation, the building architecture and the steady-state wind conditions, i.e. the incidence and the velocity.

However, it has already been underlined for natural configurations that the wind turbulence creates strong variations of the naturally ventilated flow rates, which can lead to instantaneous reversal flow rates [22]. Similar transient phenomena have been identified for both reference industrial cases, leading to a transient loss of the containment inside facilities. As an example, Figure 10 presents the time variation of the external pressure on the external leak of room B, the pressure difference through the leak and the corresponding leakage flow rate, obtained for a wind velocity fluctuating between 27 m/s and 29 m/s with configuration I. Note that the full-scale time is strongly increased due to the time scale defined from the methodology. Thus, to avoid misinterpretation of the turbulence effects due to the large full-scale time, these transient phenomena have then been studied by considering reversal time percentages, representing the ratio between the duration of negative flow rates and the total time.

Figure 10 shows that velocity variations between 27 m/s and 29 m/s generate strong variations of the external pressure field around the external architecture of the building, which lead to strong fluctuations of the internal flows and more particularly of the leakage flow rates. Thus, in the event of high variations of the instantaneous flow rates compared with the corresponding mean values, instantaneous inversions are observed even though the mean flow rate is positive. These instantaneous inversions lead to unsteady losses of the containment that should not be identified from the steady-state analysis.

To quantify in which cases these inversions occur, reversal time percentages are presented as a function of the mean leakage flow rates for each leak and each test carried out depending on the wind conditions, namely the wind velocity and the wind incidence, and the operation of the mechanical ventilation. These reversal time percentages can be estimated from the instantaneous flow rates or directly from the pressure measurements across the perforated plates, which enable to avoid potential factors affecting the transient flow rate measurements [29].

As an example, Figure 11 presents the reversal time percentages for the external leaks obtained for tests carried out on configuration I with the mechanical ventilation on. The nominal mean and the null values are presented by a red and a black dashed line, respectively. The reversal time percentage, defined as the ratio between the duration of negative flow rates and the total time, is null when the instantaneous flow remains positive and equal to 100 % when the inversion occurs during the total time of the test.

Figure 11 shows that many leakage flow rates fluctuate between negative and positive values. The analysis of these results is mainly important for positive mean flow rates, because the non-zero percentages associated with a positive mean flow rate correspond to instantaneous inversions, which have not been identified from the steady-state analysis [1]. On the contrary, the percentages lower than 100 % associated with a negative mean flow rate correspond to inversions already underlined from the steady-state analysis, although these do not occur throughout the total time.

In general, it can be concluded that the instantaneous reversal flow rates are observed when the mean flow rates are lower than the nominal flow rates. In addition, when the mean flow rates are higher than the nominal flow rates, some inversions are also identified for the external leaks, when these are located in a largely depression field, as for the leakage of room B for a wind incidence of 180° (Figure 11).

Similar analyses have been performed for the configuration II, less influenced by wind effects, with the mechanical ventilation on or off. Considering the mechanical ventilation off, Figure 12 gives the corresponding reversal time percentages and notably shows that wind turbulence also affects, to a lesser extent, the most hazardous room in terms of contamination (room D). For a wind incidence of 90°, the mean flow rates of the internal leaks are positive but associated with non-zero time percentages, approximately equal to 10 % for room D. Thus, the containment of this room is no longer always maintained and a potential pollutant can reach room A, which is directly linked to the outside. However, for this incidence, the containment of room A is completely maintained, as the external mean leakage flow rate remains positive and the time percentage equal to zero.

This experimental analysis of wind turbulence influence on the pollutant containment underlines the fact that wind turbulence must be considered when assessing the safety of industrial buildings and thus transient simulations have been carried out with the SYLVIA code to check its ability to take into account unsteady wind effects.

4.2.2. Comparison of numerical and experimental results

To take into account wind effects with the SYLVIA code, it has been shown from the steady-state study that the external pressure field on the external communications of the facility must be known and defined as boundary conditions [1]. For transient simulations, the external pressure field is also used as boundary conditions by considering the time variations of the external pressures as presented in Figure 10.

Note that for rigorously studying transient flows inside ventilation systems, the ventilation system inertia should theoretically be considered. Thus, simulations were carried out with and without considering the inertia of the ventilation system, although the parametrical study performed on the simplified cases highlights that inertia can be neglected as soon as the airflow resistance is high, such as for mechanically ventilated buildings. Figure 13 compares experimental and numerical values of the unsteady leakage flow rates of room B, corresponding to the example given in Figure 10.

Figure 13 shows that experimental and numerical results are in good agreement, even if some differences are identified when the flow rate gradient is high. Note that a sensitivity analysis of the time step was performed and led to the same results. As for the steady-state analysis [1], the highest differences are identified for low flow rates, for which the experimental uncertainties are dominant. Flow rates are determined from pressure measurements carried out with PSI sensors with pressure uncertainties considered as ±2.5 Pa. Moreover, note that only fluctuations generated by the wind turbulence are modelled, although low internal variations are also generated by the fans of the ventilation system. Thus, in spite of some differences similar to those identified for steady flows [1], the global evolutions of pressures and flow rates can be determined with the SYLVIA code.

In addition, Figure 13 shows that numerical results obtained with and without inertia are very close and thus the inertia of branches can be neglected. In general, for all the tests studied considering wind turbulence fluctuations, no significant influence of the inertia has been underlined. Neglecting ventilation system inertia means that the conservation of the branch section area and branch length scales is no longer necessary to ensure airflow similarity and leads to considering only one geometrical reduction, namely the room volume scale. Consequently, Eq. 10, which imposes a volume distortion between branches and rooms resulting from the conservation of the dimensionless parameter N_2, can be neglected. Similar conclusions have been obtained for naturally ventilated cases [21], for which experimental results obtained on models designed with and without considering the volume distortion are very close, and thus experiments were then performed without considering the volume distortion [22].

In addition, it can be concluded that the ventilation system inertia can be neglected for studying wind turbulence effects on mechanically ventilated buildings, characterized by properties (inertia, airflow resistances) with similar orders of magnitude, as well as similar boundary and initial conditions. Note that wind turbulence effects were studied on both configurations for mean wind velocities from 15 to 42 m/s and considering the ventilation system on and off. For practical considerations of designing reduced-scale models, this

conclusion means that branch section areas and branch lengths can be fixed arbitrarily, as soon as the control dampers, used to adjust head losses, ensure the conservation of airflow resistances and the inertia influence on transient airflows remains negligible.

4.3. Internal overpressure effects

Internal overpressures could also occur inside industrial facilities resulting from several accidental scenarios, such as a pressure tank fracture or a pressure peak during a fire ignition. These scenarios should be taken into account when assessing the safety of nuclear facilities and the SYLVIA code must be able to predict the transient airflow consequences of such an accident. Thus, internal overpressures have been studied, firstly, to analyse the pollutant containment of a reference industrial configuration subjected to combined wind and internal overpressure effects, secondly to check the ability of the SYLVIA code for modelling these transient phenomena and finally to identify whether the ventilation system inertia could have an influence and must be considered for such a case.

Tests were carried out on the most representative configuration of nuclear facilities, namely configuration II, concerned by such accidental scenarios. Internal overpressures, of approximately 2500 Pa at the full scale, have been generated inside the most hazardous room of configuration II (room D) by using an air valve controller connected to the pressure air plant of the laboratory.

4.3.1. Results obtained with the mechanical ventilation on

Figure 14 compares experimental and numerical internal room pressures for an internal overpressure generated inside room D with the mechanical ventilation on and without wind. Here again, full-scale results are considered by applying the corresponding pressure and time scales to the reduced-scale results, explaining the large duration of the overpressure.

Concerning the pollutant containment, Figure 14 shows that the hierarchy of depressions between rooms is not completely reversed during the internal overpressure: due to the pressure difference between rooms A and B which is always positive during the overpressure, the internal leakage flow rate remains positive and prevents a potential contamination of room A through leakages. However, for other tests performed by simultaneously considering internal overpressure and external negative pressure on the external leak of room A due to wind effects (e.g. for an incidence of 0°), a complete inversion of the depressions was obtained. Moreover, a reversal flow rate inside the blowing duct of the source room (room D) was always identified during internal overpressures and leads to a potential release of a gaseous pollutant inside room A through the blowing ventilation system. This result underlines the importance of the HEPA filter located inside the blowing branch of the source room, which prevents particle dispersion inside the ventilation system.

Figure 14 also shows that the numerical results correctly fit with the experimental results. The differences identified are similar to those identified for steady flows and mainly arise from experimental uncertainties [1]. In addition, numerical results obtained with and without considering the ventilation system inertia are very close, meaning that inertia can be neglected

for the configuration studied. Moreover, no significant temporal phases have been identified between the source room (room D) and all of the other measurement points, implying that internal overpressure propagation can be considered as instantaneous. Thus, transient evolutions of pressures and flow rates can be assumed as quasi-steady flows, supporting that transient differences between experimental and numerical results are similar to steady-state differences.

4.3.2. Results with the mechanical ventilation off

Figure 15 compares experimental and numerical room pressures for an internal overpressure generated when no steady flow is initially established inside the configuration, i.e. when the mechanical ventilation is off and no wind effect is considered. This case, without initial steady flows, is the only one for which it has been underlined that the ventilation system inertia has an influence.

First, knowing that the hierarchy of depressions is no longer ensured because the ventilation is off, the internal overpressure inside room D logically propagates to the other rooms. Figure 15 shows that numerical evolutions obtained with and without considering inertia are not rigorously identical during the overpressure. To illustrate this, Figure 16 presents results for the three evolutions on which the inertia influence is the most significant, namely the leakage flow rate between rooms A and B, resulting from the room pressures given in Figure 15, the general blowing pressure and the chimney pressure.

These results show that overshoots are identified before reaching the steady-state values during the increase or decrease of the overpressure. These overshoot phenomena are numerically reproduced only for simulations carried out by considering the ventilation system inertia. Thus, these numerical results with inertia are closer to experimental results than those obtained without inertia, even if deviations are identified due to the high experimental uncertainties for low pressure and flow rate values obtained without mechanical ventilation and wind effects.

By analogy with parametrical results obtained for simplified cases (section 3.3), these overshoots correspond to Helmholtz oscillations associated with a high damping ratio. It has been concluded from parametrical simulations (section 3.3) that the damping ratio is proportional to the airflow resistance, explaining its high value for configurations with a ventilation system.

These conclusions have been supported by carrying out some numerical simulations on the configurations II by considering a theoretical pressure step and modifying the ventilation system inertia. These simulations show that even if the dynamics of the transient pressure is strongly increased, i.e. that the pressure step is generated in 1 s, similar phenomena are observed. No inertia influence was observed for the case with the ventilation on whereas overshoot corresponding to oscillations with a high damping ratio were identified for the case without initial steady flows (i.e. with the ventilation system off and without wind effects). Thus, further work is still needed to characterize the influence of initial steady flows on transient airflow behaviour.

In addition, it has been numerically shown that in order to obtain oscillations inside this configuration, the ventilation system inertia must be multiplied by 10, which is no longer representative of real configurations. In this case, oscillations with lower damping ratio and oscillation frequency are identified. This result agrees with the parametrical results presented in section 3 (cf. Figure 8). Although an explicit relation between ventilation system inertia and oscillations frequency cannot be easily determined for an entire mechanically ventilated buildings, the oscillation frequency remains proportional to the square root of the inverse of the inertia as for the simplified cases (Eqs. 12 and 13). This result supports the correspondence between Helmholtz oscillations and overshoot obtained on the reference industrial configuration II. Thus, following an accidental overpressure, no strong Helmholtz oscillations may be identified on industrial buildings equipped with ventilation systems, due to its inertia and high airflow resistances.

Finally, except for the case presented above without initial steady flows, the inertia of the ventilation system can be neglected, provided that the inertia values are representative of real ventilation systems. Thus, as for the wind turbulence study (section 4.2), the scaling down methodology can be greatly simplified: no branch section area and length scales should be defined and the conservation of the dimensionless parameter N_2 implying the volume distortion between rooms and branches make no sense since branch inertia is neglected.

5. Conclusions and perspectives

Transient flows have been experimentally and numerically studied on simplified cases and reference industrial configurations representative of industrial facilities. Reduced-scale experiments are based on the scaling down methodology developed, which makes it possible to reproduce by similarity steady and transient internal airflows inside buildings equipped with ventilation systems [1]. The particularity of this methodology consists in introducing a volume distortion between the room volume and the branch volume of the ventilation system in order to reproduce internal oscillations corresponding to Helmholtz oscillations that could occur, by analogy with the reduced-scale approach developed for a naturally ventilated single room with a large opening [3-4].

This Helmholtz oscillated phenomenon has been observed mainly on the simplified cases studied, which are not representative of industrial configurations equipped with ventilation systems. Thus, in these simplified cases, it has been highlighted that considering volume distortion and branch inertia is fundamental to perfectly reproduce internal transient evolutions of pressures and flow rates. On the contrary, it has been highlighted in the reference industrial cases that the ventilation system inertia can almost always be negligible and the transient flows can be assumed as quasi-steady flows, both for studying external transient flows due to wind turbulence and internal transient flows resulting from accidental overpressures. The only case for which the ventilation system inertia has an influence has been identified when no initial steady flow is established, i.e. with the mechanical ventilation off and without wind effects. In this case, Helmholtz oscillations associated with a high damping ratio due to the high airflow resistance are observed. Thus, except for this case, it has been concluded that the scaling down methodology can be greatly simplified by considering

only geometrical reduction for the rooms. The ventilation system sizes can be defined arbitrarily, as long as the corresponding inertia is not considerably higher than the inertia of real ventilation systems and the control dampers make it possible to adjust the head losses in order to ensure the airflow resistance similarity.

Concerning the ability of the SYLVIA code for modelling transient flows, all the experimental results obtained on simplified and reference cases have been compared with numerical results. It has notably been shown that the SYLVIA code perfectly reproduces the Helmholtz oscillations identified in the simplified cases studied. In addition, for industrial configurations, it has been shown that the SYLVIA code can take into account wind turbulence and internal overpressure effects, without considering the ventilation system inertia, the influence of which remains very low. The ability of the SYLVIA code to simulate these transient effects is fundamental for supporting nuclear safety assessments, because it has been highlighted that pollutant containment can be lost, notably with the turbulence effects that imply unsteady flow rate inversions which cannot be identified when only considering mean airflows. However, the main difficulty will be the definition of the external pressure generated by wind that needs to be used as boundary conditions.

Finally, the main perspective of this work is to extend the scaling down methodology to consider transfers due to thermal effects, which may arise during an accident such as a fire. A research project is thus currently beginning to study mass transfers due to thermal effects inside industrial buildings equipped with ventilation systems.

6. References

[1] Le Roux N, Faure X, Inard C, Soares S, Ricciardi L. Reduced-scale study of wind influence on mean airflows inside buildings equipped with ventilation systems. Building and Environment 2012; 58:231-244

[2] Audouin L, Chandra L, Consalvi JL, Gay L, Gorza E, Hohm V, Hostikka S, Ito T, Klein-Hessling W, Lallemand C, Magnusson T, Noterman N, Park JS, Peco J, Rigollet L, Suard S, Van-Hees P. Quantifying differences between computational results and measurements in the case of a large-scale well-confined fire scenario. Nuclear Engineering and Design 2011; 241:18–31

[3] Holmes JD. Mean and fluctuating internal pressures induced by wind. Proceedings of the Fifth International Conference on Wind Engineering 1979; 435–450.

[4] Holmes JD, Ginger JD. Internal pressures – The dominant windward opening case – A review. Journal of Wind Engineering and Industrial Aerodynamics 2012; 100:70-76.

[5] Etheridge DW. Unsteady flow effects due to fluctuating wind pressures in natural ventilation design – Mean flow rates. Building and Environment 2000; 35:111-133.

[6] Etheridge DW. Unsteady flow effects due to fluctuating wind pressures in natural ventilation design – Instantaneous flow rates. Building and Environment 2000; 35:321-337.

[7] Mariaux G. Etude du comportement dynamique des circuits aérauliques : Application au contrôle actif des variations rapides de pression dans les trains à grandes vitesses. PhD Thesis, University of Poitiers; 1995.

[8] Vickery BJ. Gust factors for internal pressures in low rise buildings. Journal of Wind Engineering and Industrial Aerodynamics 1986; 23:259-271

[9] Liu H, Saathoff PJ. Building Internal Pressure: Sudden Change, Journal of the Engineering Mechanics Division, ASCE, 1981; 107:309-321

[10] Liu H, Rhee KH. Helmholtz oscillation in buildings model, Journal of Wind Engineering and Industrial Aerodynamics 1986; 24:95-115

[11] Sharma RN, Richards PJ. Computational modelling of the transient response of building internal pressure to a sudden opening, Journal of Wind Engineering and Industrial Aerodynamics 1997; 72:149-161

[12] Sharma RN., Richards PJ. The influence of Helmholtz resonance on internal pressures in a low-rise building, Journal of Wind Engineering and Industrial Aerodynamics 2003; 91:807-828

[13] Oh JH, Kopp GA, Inculet DR. The UWO contribution to the NIST aerodynamics database for wind loads on low buildings: Part 3. Internal Pressure. Journal of Wind Engineering and Industrial Aerodynamics 2007; 95:755-779.

[14] Vickery BJ, Bloxham C. Internal pressure dynamics with a dominant opening, Journal of Wind Engineering and Industrial Aerodynamics 1992; 41-44, 193-204

[15] Woods AR, Blackmore PA. The effect of dominant openings and porosity on internal pressures, Journal of Wind Engineering and Industrial Aerodynamics 1995; 57:167-177

[16] Pearce W, Sykes DM. Wind tunnel measurements of cavity pressure dynamics in a low-rise flexible roofed building, Journal of Wind Engineering and Industrial Aerodynamics 1999; 82:27-48

[17] Ho TCE, Surry D, Morrish D, Kopp GA. The UWO contribution to the NIST aerodynamic database for wind loads on low buildings: Part 1. Archiving format and basic aerodynamic data. Journal of Wind Engineering and Industrial Aerodynamics 2005; 93:1-30

[18] Stathopoulos T, Luchian HD. Transient wind-induced internal pressures, Journal of Engineering Mechanics 1989; vol. 115, No. 7, 1501-1514

[19] Sharma RN. Internal and net envelope pressures in a building having quasi-static flexibility and a dominant opening. Journal of Wind Engineering and Industrial Aerodynamics 2008; 96:1074-1083.

[20] Guha TK, Sharma RN, Richards PJ. Internal pressure dynamics of a leaky building with a dominant opening. Journal of Wind Engineering and Industrial Aerodynamics 2011; 99:1151-1161

[21] Chiu YH. Development of Unsteady Design Procedures for Natural Ventilation Stacks. PhD Thesis, University of Nottingham; 2004

[22] Wang B, Etheridge DW, Ohba M. Wind tunnel investigation of natural ventilation through multiple stacks. Part 2: Instantaneous Values. Building and Environment 2011; 46:1393-1402

[23] AHSRAE. ASHRAE Handbook: Fundamentals. SI ed. American Society of Heating, Refrigerating and Air-Conditioning Engineers Inc; 2001, p.26.1-26.32

[24] Walker IS, Wilson DJ, Sherman MH. A comparison of the power law to quadratic formulations for air infiltration calculations. Energy and Buildings 1998; 27, 293-299

[25] AFNOR. Distribution et diffusion d'air – Technique de mesure du débit d'air dans un conduit aéraulique. Standard NFX 10-231; 1984

[26] Solliec C. Simultaneous measurements of fluctuating pressures using piezoresistive multichannel transducers as applied to atmospheric wind tunnel tests. Journal of Wind Engineering and Industrial Aerodynamics 1995 ; 56:71-86

[27] Le Roux N. Etude par similitude de l'influence du vent sur les transferts de masse dans les bâtiments complexes. PhD Thesis, University of La Rochelle; 2011

[28] Le Roux N, Faure X, Inard C, Soares S, Ricciardi L. Dimensional analysis of ventilation systems to study isothermal flows in steady and transient conditions. 10th REHVA world congress CLIMA 2010, Antalya, Turkey; 2010

[29] Doblhoff-Dier K, Kudlaty K, Wiesinger M, Gröschl M. Time resolved measurement of pulsating flow using orifices. Flow Measurement and Instrumentation 2011; 22:97-103

Highlights

Transient flows in ventilation systems were experimentally and numerically studied.
Helmholtz oscillations have been characterized depending on branch characteristics.
The ventilation system inertia can often be negligible for industrial cases studied.
Wind turbulence can lead to unsteady losses of the containment inside buildings.
The Sylvia code has been validated for taking into account transient flow phenomena.

Table 1: Relations between fixed and calculated scale parameters [1].

Fixed scale parameters	Calculated scale parameters		
$\overline{V}$	$\overline{S} = \frac{\overline{Q}}{\overline{U}}$	$\overline{P} = \overline{U}^2$	$\overline{R_{duct}} = \frac{1}{\overline{S}^2}$
$\overline{U}$			$\overline{R_{filter}} = \frac{\overline{U}}{\overline{S}}$
$\overline{Q}$	$\overline{L} = \frac{\overline{V}\overline{U}^2}{\overline{S}}$	$\overline{t} = \frac{\overline{L}}{\overline{U}}$	$\overline{R_{leak}} = \frac{\overline{U}^{2-n}}{\overline{S}^n}$

Table 2: Inertial properties of the experimental models studied.

	Length (m) $L_1 – L_2$	**Diameter (mm)** $D_1 – D_2$	**Inertia (kg.m^{-4})** $I_1 – I_2$
Reference-scale model	2.24	192	92
Reduced-scale model	0.8	44	626
Inertial reference-scale model	26.5 – 2.24	78 – 192	6600 – 92
Inertial reduced-scale model n°1	5 – 0.8	25 – 44	12120 – 626
Inertial reduced-scale model n°2	15 – 0.8	25 – 44	36360 – 626

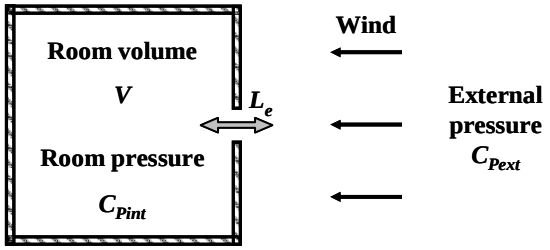

Figure 1: Helmholtz resonator model of internal pressure fluctuations (Holmes et al., [4]).

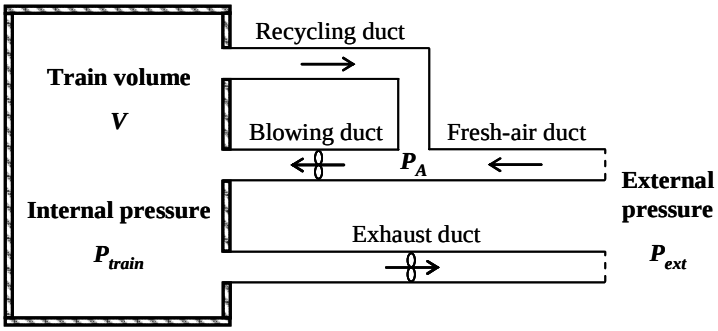

Figure 2: Simplified view of the train ventilation system studied by Mariaux [7].

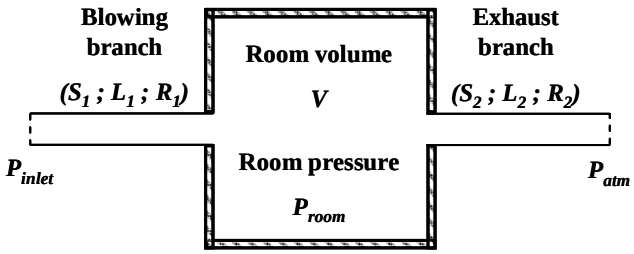

Figure 3: Diagram of the simplified cases studied.

Figure 4: View of the reference-scale and the reduced-scale models (top) and view of the "inertial" reference-scale (bottom left) and reduced-scale (bottom right) models.

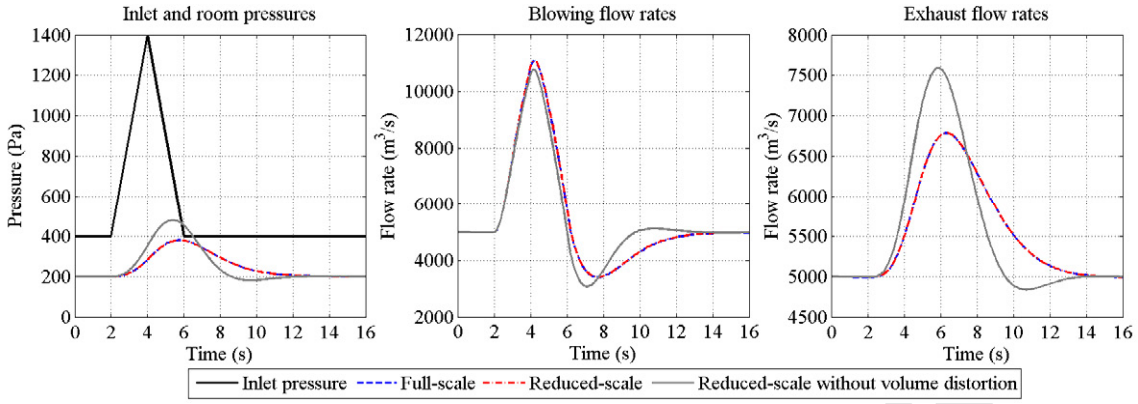

Figure 5: Full-scale comparison of room pressures, blowing and exhaust flow rates obtained at the full-scale and the reduced-scale with and without considering the volume distortion.

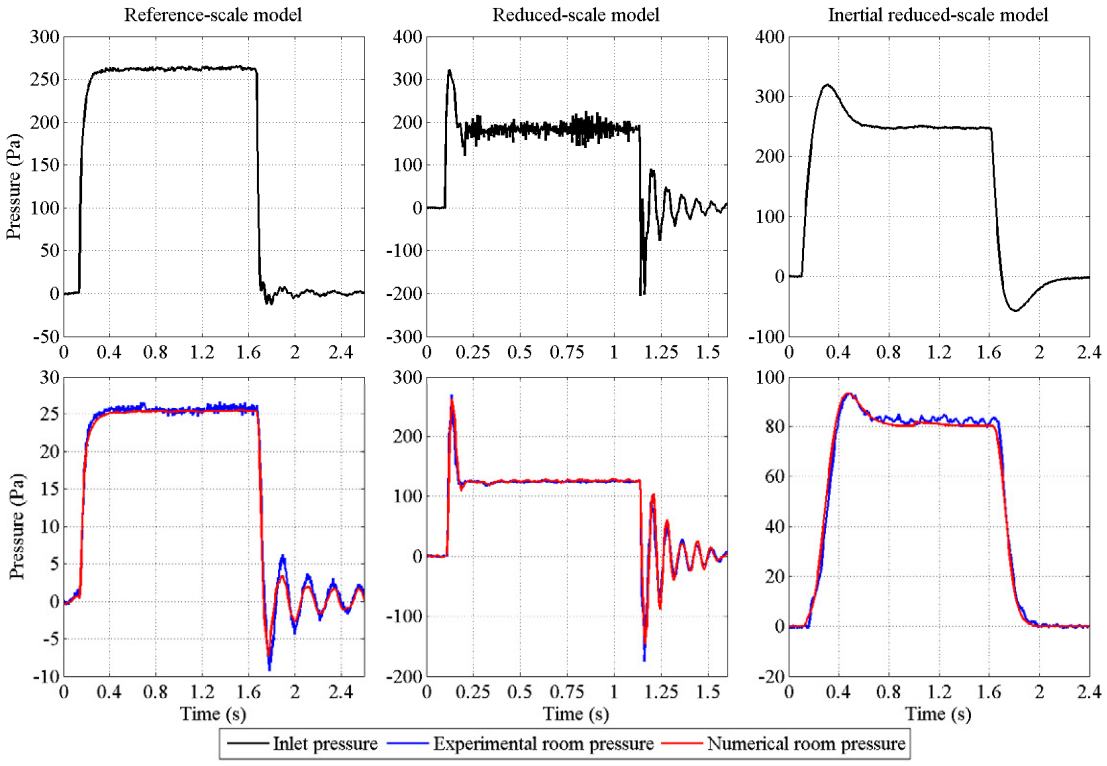

Figure 6: Comparison of experimental and numerical room pressures for three models, subjected to an inlet overpressure (left: reference-scale model; centre: reduced-scale model; right: inertial reduced-scale model n°2).

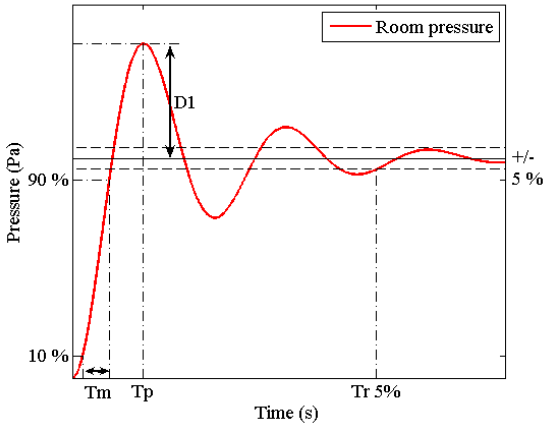

Figure 7: Characteristic quantities of a pseudo-periodic evolution of the internal room pressure.

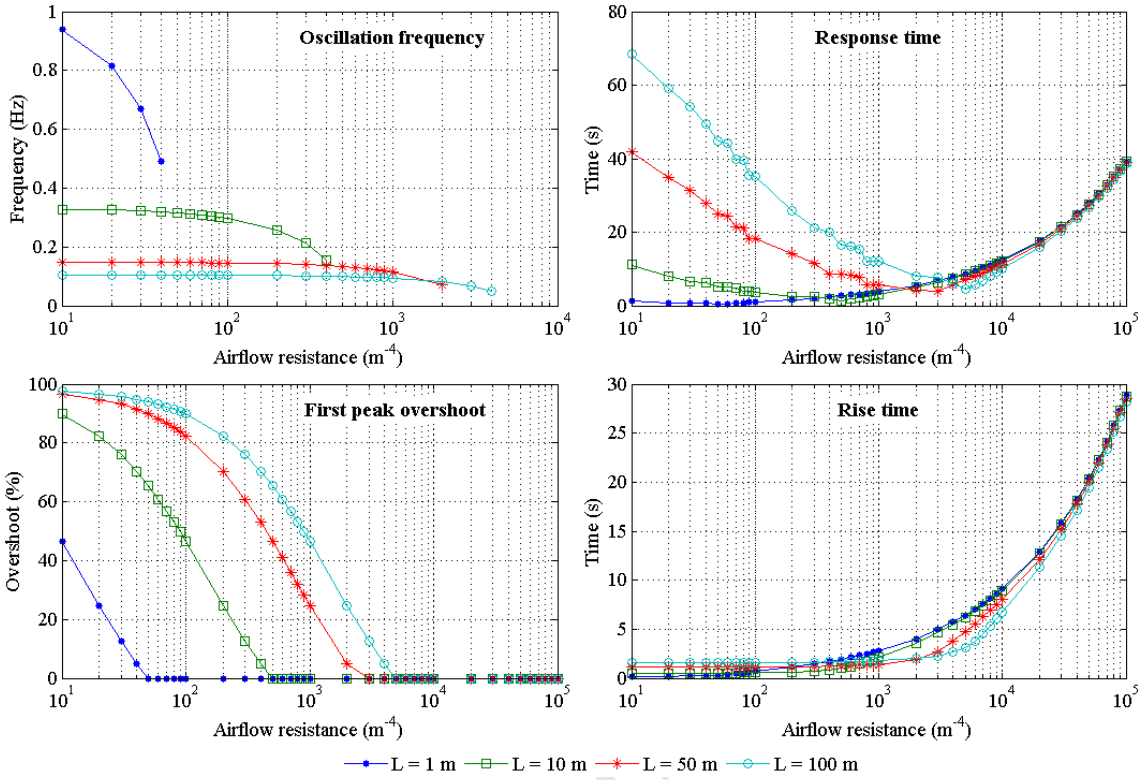

Figure 8: Characteristic quantities of the time response of the system with similar blowing and exhaust quadratic branches.

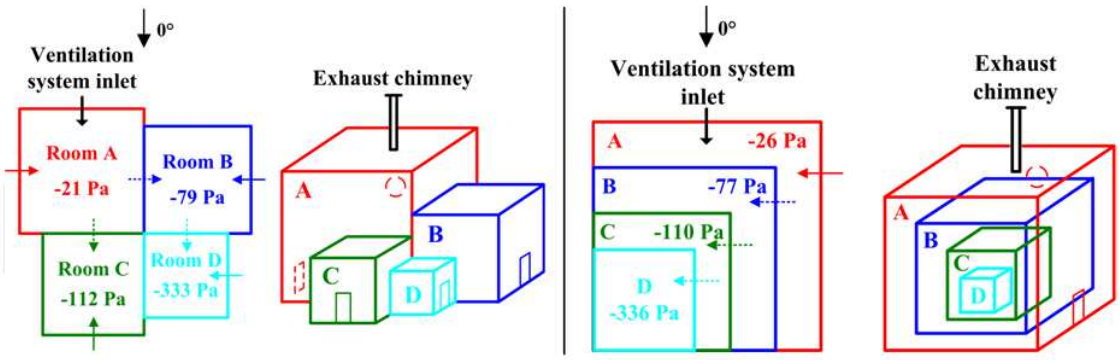

Figure 9: Building architectures of reference industrial configurations studied (left: configuration I – right: configuration II).

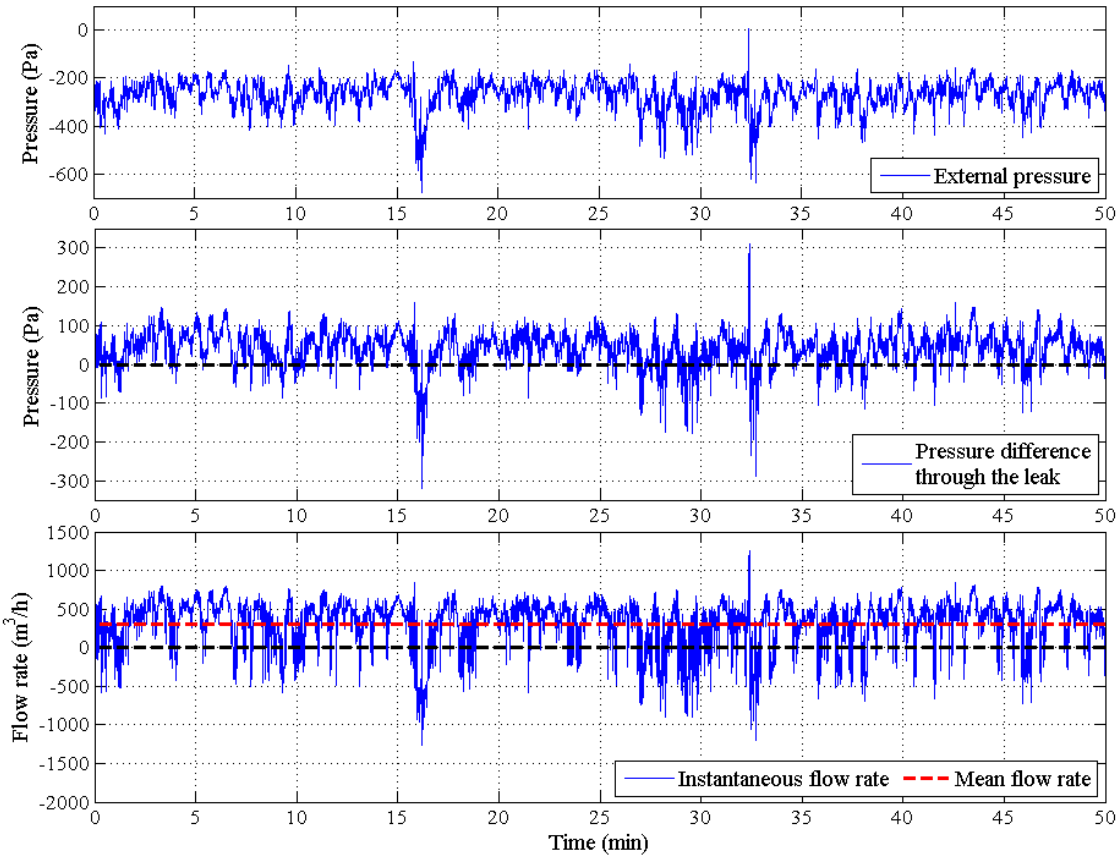

Figure 10: Time variations of the external pressure on the leak of room B, the pressure difference through the leak and the corresponding leakage flow rate (mechanical ventilation on, wind velocity between 27 m/s and 29 m/s, wind incidence of 0°, configuration I).

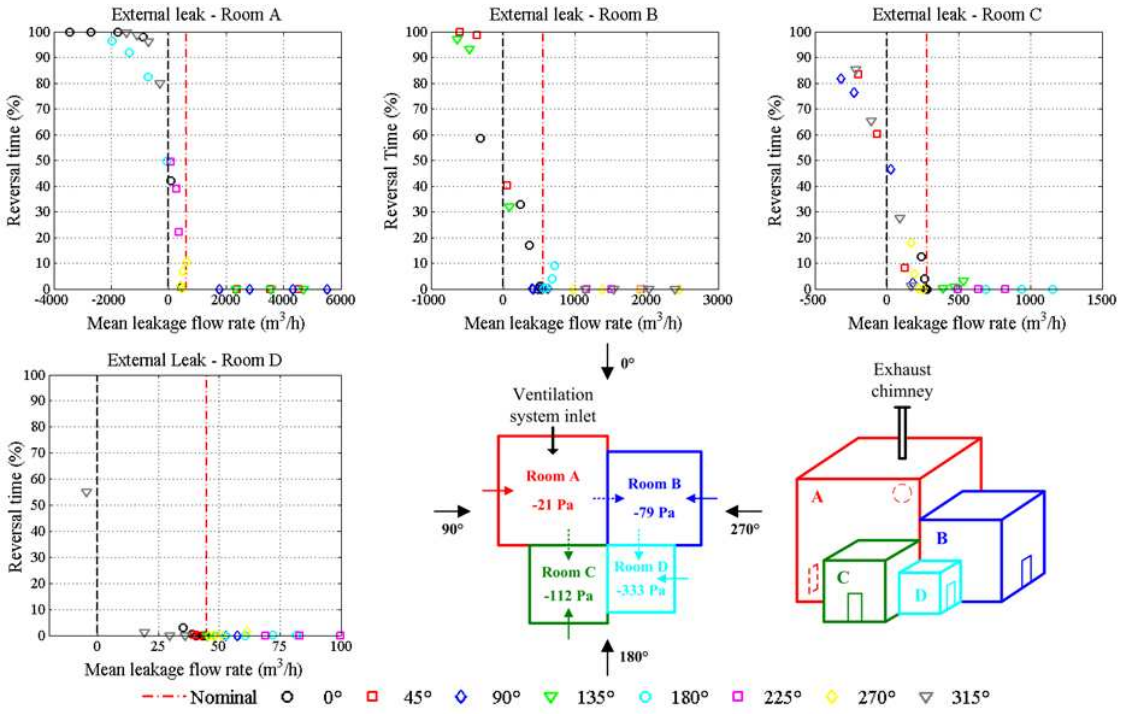

Figure 11: Reversal time percentages of the instantaneous external leakage flow rates, as a function of the mean leakage flow rates (mechanical ventilation on, configuration I).

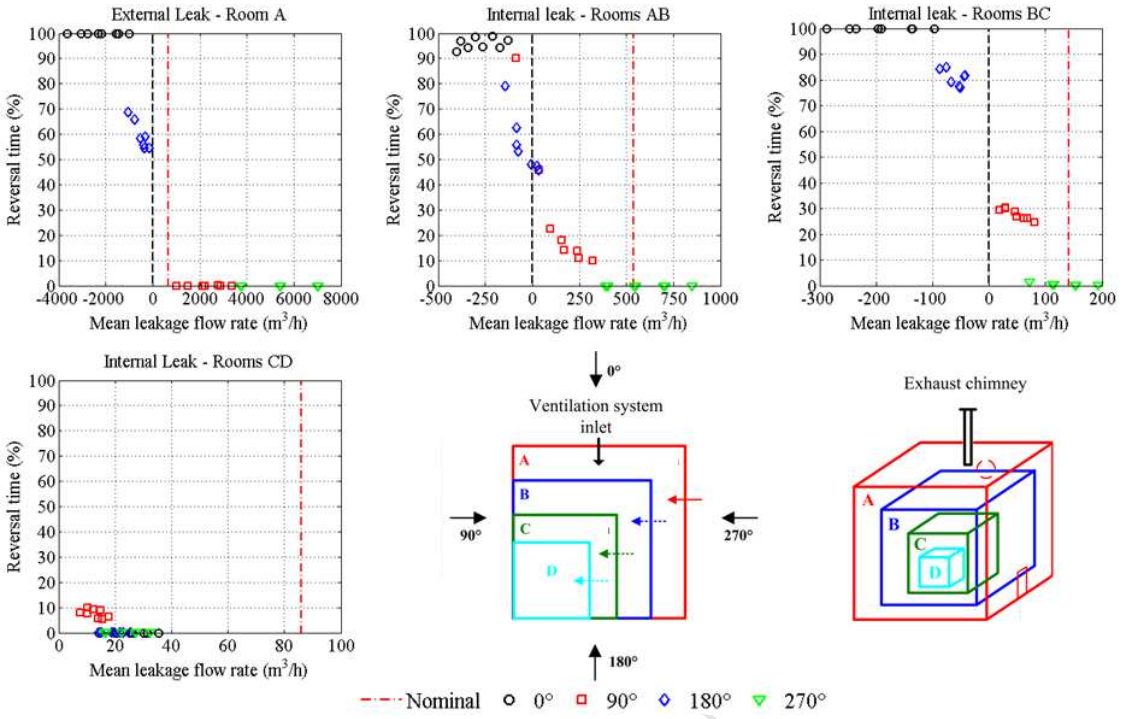

Figure 12: Reversal time percentages of the instantaneous leakage flow rates, as a function of the mean leakage flow rates (mechanical ventilation off, configuration II).

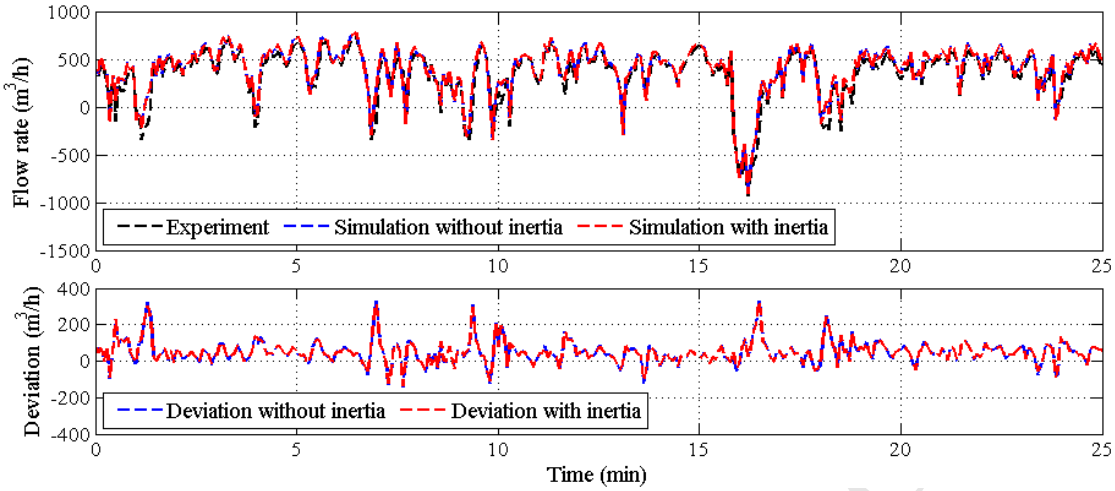

Figure 13: Comparison of experimental and numerical values of the unsteady leakage flow rate of room B (mechanical ventilation on, wind velocity between 27 m/s and 29 m/s, wind incidence of 0°, configuration I).

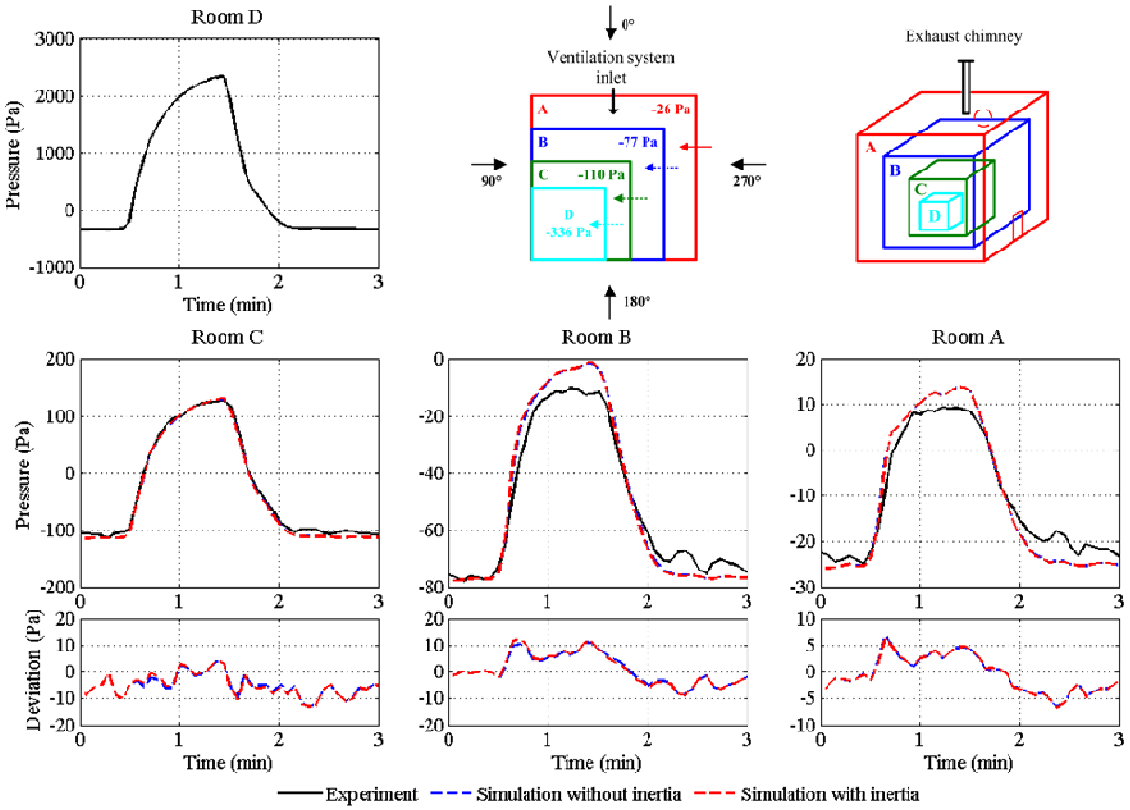

Figure 14: Experimental and numerical comparisons of internal room pressures (internal overpressure inside room D, without wind, ventilation system on).

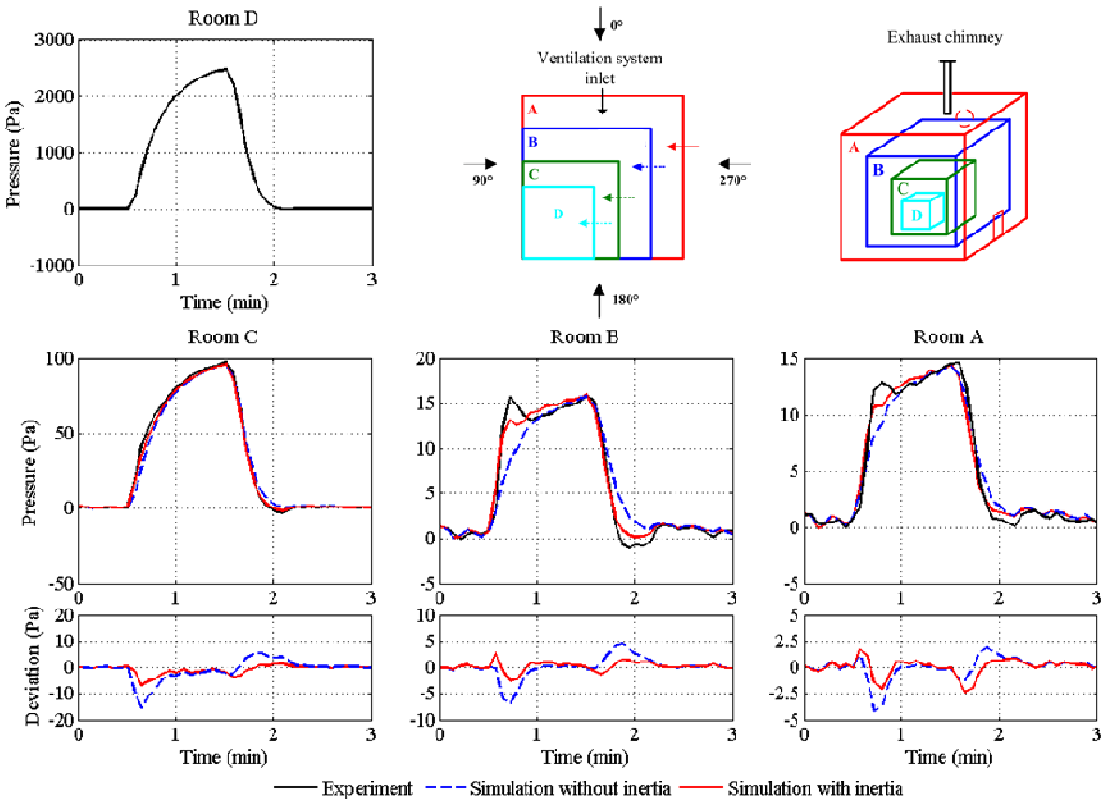

Figure 15: Experimental and numerical comparisons of internal room pressures (internal overpressure inside room D, without wind, ventilation system off).

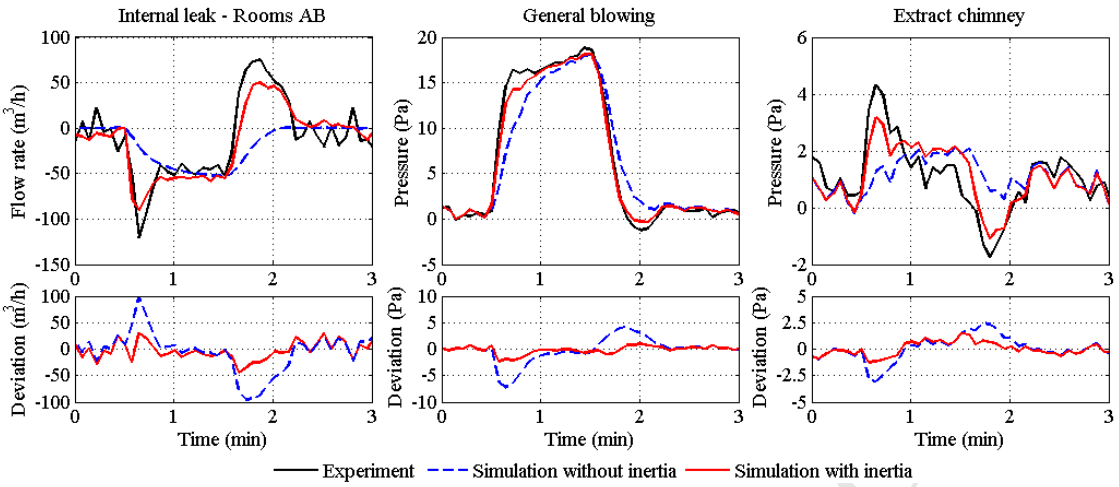

Figure 16: Experimental and numerical comparisons for the most influenced evolutions (internal overpressure inside room D, without wind, ventilation system off).